JOURNAL OF BACTERIOLOGY, Oct. 1990, p. 5575–5585
0021-9193/90/105575-11$02.00/0

Vol. 172, No. 10

Similar Organization of the *sigB* and *spoIIA* Operons Encoding Alternate Sigma Factors of *Bacillus subtilis* RNA Polymerase

SUE KALMAN,† MARIAN L. DUNCAN, SUSAN M. THOMAS, AND CHESTER W. PRICE*
Department of Food Science and Technology, University of California, Davis, California 95616

Received 28 February 1990/Accepted 17 July 1990

Bacillus subtilis **sigma-B is an alternate sigma factor implicated in controlling stationary-phase gene expression. We characterized the genetic organization and regulation of the region containing the sigma-B structural gene (*sigB*) to learn which metabolic signals and protein factors govern sigma-B function. *sigB* lay in an operon with four open reading frames (orfs) in the order orfV-orfW-*sigB*-orfX, and *lacZ* gene fusions showed that all four frames were translated in vivo. Experiments with primer extension, S1 nuclease mapping, and *lacZ* transcriptional fusions found that *sigB* operon transcription initiated early in stationary phase from a site 32 nucleotides upstream of orfV and terminated 34 nucleotides downstream of orfX. Fusion expression was abolished in a strain carrying an in-frame deletion in *sigB*, suggesting that *sigma-B* positively regulated its own synthesis, and deletions in the *sigB* promoter region showed that sequences identical to the sigma-B-dependent *ctc* promoter were essential for promoter activity. Fusion expression was greatly enhanced in a strain carrying an insertion mutation in orfX, suggesting that the 22-kilodalton (kDa) orfX product was a negative effector of sigma-B expression or activity. Notably, the genetic organization of the *sigB* operon was strikingly similar to that of the *B. subtilis spoIIA* operon, which has the gene order *spoIIAA-spoIIAB-spoIIAC*, with *spoIIAC* encoding the sporulation-essential sigma-F. The predicted sequence of the 12-kDa orfV product was 32% identical to that of the 13-kDa SpoIIAA protein, and the 18-kDa orfW product was 27% identical to the 16-kDa SpoIIAB protein. On the basis of this clear evolutionary conservation, we speculate these protein pairs regulate their respective sigma factors by a similar molecular mechanism and that the *spoIIA* and *sigB* operons might control divergent branches of stationary-phase gene expression.**

Alternate sigma factors associate with the catalytic core of procaryotic RNA polymerases to reprogram the pattern of gene expression in response to nutritional or environmental stress or, in some cases, in response to morphological change. Examples include regulation of the heat shock and nitrogen regulons of enteric bacteria (14, 22, 23, 44, 47), regulation of the chemotaxis and motility regulons of enteric bacteria and *Bacillus subtilis* (1, 16), and regulation of developmental gene expression in *B. subtilis* and *Streptomyces coelicolor* (5, 20, 21, 27, 46). However, it is not well understood how cellular and metabolic signals command the transcriptional apparatus to modulate gene expression.

In the best-studied example, the NtrA sigma factor of enteric bacteria is controlled at the level of activity, not synthesis. The NtrA sigma determines promoter specificity for genes of diverse function, and it is a two-component regulatory system that controls activation of the closed initiation complex (22). For nitrogen-regulated promoters in *Escherichia coli* and *Salmonella typhimurium*, this two-component activation system responds to an elegant metabolic cascade which signals nitrogen availability (44). In contrast, the rate of transcription initiation at enteric heat shock promoters is regulated by changes in the intracellular concentration of the heat shock sigma factor HtpR, whose synthesis appears to be controlled primarily at the posttranscriptional level (47). The channel linking the signal of physiological stress to heat shock sigma synthesis is unknown. These two examples hint that considerable diversity is likely in the mechanisms regulating sigma factor synthesis and activation.

* Corresponding author.
† Present address: Sandoz Crop Protection, Palo Alto, CA 94304.

At least nine different sigma factors associate with *B. subtilis* RNA polymerase (20, 21, 27, 49). Many of these control the sporulation process via a cascade mechanism first proposed by Losick and Pero (26). However, sporulation-specific gene expression is only part of stationary-phase metabolism, which includes adaptation to the growth-limiting stress, development of competence, induction of chemotaxis and motility, and synthesis of antibiotics and extracellular enzymes (41). Other likely stationary-phase events include activation of genes essential for survival under nonsporulating conditions and activation of genes required for return to vegetative phase when favorable growth conditions arise before the cell is committed to sporulation. The mechanisms and signals which control the alternate sigma factors and which integrate regulation of stationary-phase gene expression are largely unknown.

Sigma-B (formerly sigma-37) is an alternate sigma factor of *B. subtilis* RNA polymerase which is not essential for sporulation (2, 9, 18). Rather, sigma-B is required for maximal expression of *ctc* and *csbA*, two genes of unknown function which are transcribed in early stationary phase under conditions inimical to sporulation (18, 19; S. A. Boylan, M. D. Thomas, and C. W. Price, unpublished data). Understanding the metabolic signals and protein factors which govern expression of the sigma-B structural gene (*sigB*) and the activity of sigma-B holoenzyme should elucidate some of the mechanisms regulating alternate sigma factors in stationary phase.

We report here that *sigB* is the third cistron of a four-gene operon, that the products of the last two genes autoregulate operon expression, and that the products of the first two genes have sequences very similar to those of the two genes preceding the sporulation-essential sigma-F gene in the *B. subtilis spoIIA* operon (13), suggesting that they might fulfill

TABLE 1. *B. subtilis* strains

Strain	Relevant genotype	Reference or construction[a]
PB2	Wild type	168 Marburg strain (31)
PB61	*spo0A12*	3
PB105	*sigBΔ1*	This study
PB110	*amyE*::pDH32-4	pDH32-4→PB2
PB111	*amyE*::pDH32-3	pDH32-3→PB2
PB114	*sigB*::pMD10	pMD10→PB2
PB115	*orfX*::pMD11	pMD11→PB2
PB116	*orfW*::pMD8	pMD8→PB2
PB118	*orfV*::pMD6	pMD6→PB2
PB119	*amyE*::pDH32-2	pDH32-2→PB2
PB120	*amyE*::pDH32-2R	pDH32-2R→PB2
PB121	*amyE*::pDH32-1	pDH32-1→PB2
PB122	*amyE*::pDH32-2 *sigBΔ1*	PB119→PB105
PB123	*amyE*::pDH32-2 *orfX*::*ery*	pSK15→PB119
PB148	*amyE*::pDH32-2 *spo0A12*	PB119→PB61
PB163	*amyE*::pDH32-5	pDH32-5→PB2

[a] Arrow indicates transformation, donor → recipient.

equivalent roles within their respective operons. Because the *sigB* and *spoIIA* operons have a similar genetic organization and are both expressed at approximately the same time in the early stationary phase of growth, we hypothesize that these two operons might control alternative pathways of stationary-phase gene expression.

MATERIALS AND METHODS

Bacteria, phage, and genetic methods. We used *E. coli* DH5α (Bethesda Research Laboratories) as the host for all plasmid constructions and Y1090 (52) as the host for λgt11. λgt11 bacteriophage were grown as described by Davis et al. (7). *B. subtilis* strains used are shown in Table 1. *B. subtilis* PB2 and its derivatives were hosts for natural transformations with linear and plasmid DNA as described previously (31). Transformation selections for drug-resistant *B. subtilis* strains were done on tryptose-blood-agar plates (Difco Laboratories) containing either 1 μg of erythromycin and 25 μg of lincomycin per ml or 5 μg of chloramphenicol per ml. The Amy phenotype of *B. subtilis* transformants was determined by iodine staining of tryptose-blood-agar plates containing 1% starch (40). Schaeffer 2×SG sporulation medium was described by Leighton and Doi (24), and Luria broth (LB) and M9 minimal glucose medium were from Davis et al. (7).

DNA methods. Hybridization screening of λgt11 libraries was done as described by Davis et al. (7), and all standard recombinant DNA methods were performed as described previously (4). DNA sequencing was done by the dideoxynucleotide chain termination method (37) with appropriate restriction fragments cloned into pUC18 and pUC19. We made sets of nested deletions as described previously (4) and used Sequenase enzyme (U.S. Biochemicals) and [α-^{35}S] dATP (Amersham) to label sequencing reactions primed on double-stranded DNA templates. Reaction conditions were those described by U.S. Biochemicals.

Construction of insertion and deletion mutations. We transferred a 453-base-pair (bp) in-frame deletion in the *sigB* coding region to the chromosome by the two-step allele replacement method of Stahl and Ferrari (43). pUC19 containing nucleotides (nt) 387 to 2292 of the *sigB* region was digested with *Hin*cII at nt 1100, 1465, and 1552 (see Fig. 2) and then religated. DNA sequencing across the new *Hin*cII junction confirmed that the deletion restored the correct reading frame. The plasmid insert was moved to the integration vector pCP115 (31) for allele replacement. Following plasmid insertion and excision from the chromosome of *B. subtilis* PB2, Southern blotting confirmed the presence of the deletion (*sigBΔ1*) on the chromosome. The strain carrying *sigBΔ1* was designated PB105.

We also made an insertion-deletion mutation in the open reading frame orfX. pUC19 carrying the *sigB* and orfX region was digested with *Cla*I and *Pst*I to remove a 104-bp fragment from within orfX. We replaced this deleted region with the 1,443-bp *Taq*I fragment carrying the macrolide-lincosamide-streptogramin B resistance gene from pE194 (17). The resulting construction, pSK15, was linearized and used to transform strain PB119 to erythromycin resistance. Southern blotting confirmed that the deletion-insertion construction replaced the chromosomal orfX region via a double-crossover event. The strain carrying the orfX null mutation was designated PB123.

Construction of transcriptional and translational fusions. We made two kinds of transcriptional fusions, single-copy at the *amyE* locus with the pDH32 vector (Dennis Henner, personal communication) and multicopy with the pLC4 vector (33). The *sigB* operon fragments shown in Fig. 1 were ligated into the *Eco*RI site of pDH32 and transformed into *E. coli*. Those clones with fragments in the correct orientation were linearized with *Pst*I or *Sca*I and transformed into *B. subtilis* PB2. Scoring for the Amy phenotype and Southern blotting confirmed integration at the *amyE* locus by a double crossover event. Because the 2.3-kilobase (kb) *Eco*RI fragment of pDH32-1 was apparently lethal in *E. coli*, we directly transformed the linearized pDH32-1 construction into *B. subtilis*. Southern blotting identified the transformant PB121, which carried the *lacZ* fusion in the correct orientation.

To locate sequences necessary for *sigB* operon promoter activity, we made a series of Bal31 deletion mutations of the putative promoter region. These deletion constructions were then assayed for promoter activity in the *xylE* transcriptional fusion vector pLC4. The 397-bp *Pst*I-*Aha*III fragment (nt 1 to 397 in Fig. 2) was moved into the *Pst*I and *Hin*cII sites of pUC19 to make pSK12. We linearized pSK12 at the unique *Pst*I site, digested it with Bal31 exonuclease (New England BioLabs), filled it in with the Klenow fragment of DNA polymerase to generate blunt ends, and then ligated it in the presence of *Eco*RI linkers. Following transformation of *E. coli*, two deletions of the appropriate size were identified by restriction mapping and DNA sequencing. pSK13 had 110 bp deleted downstream from the *Pst*I site, and pSK14 had 139 bp deleted. The original *Pst*I-*Aha*III fragment from pSK12 and the two deletion fragments from pSK13 and pSK14 were subcloned between the *Eco*RI and *Bam*HI sites of pLC4 to generate pLC4-400, pLC4-110, and pLC4-139, respectively. We also used pLC4 for an in vivo assay of terminator function, placing the 117-bp *Eco*RI-*Hin*cII fragment containing the putative terminator of the *sigB* operon (nt 2293 to 2409 in Fig. 2) between the 397-bp promoter-containing fragment and the *xylE* reporter gene of the plasmid. This construction was called pLC4-400T.

To determine whether the four reading frames in the *sigB* operon were expressed in vivo, single-copy translational fusions were made into each frame by using the pJF751 integration vector (11). Fragments from the *sigB* region were cloned into the *Eco*RI or *Sma*I site of pJF751 by using either *Eco*RI linkers or blunt-end ligation. Fragments cloned were: orfV, the 183-nt *Acc*I-*Sau*3A fragment (nt 270 to 453 in Fig. 2) to make pMD6; orfW, the 312-nt *Rsa*I-*Hgi*AI fragment (nt 367 to 679) to make pMD8; *sigB*, the 732-nt *Rsa*I-*Hin*cII fragment (nt 367 to 1099) to make pMD10; and orfX, the

731-nt *Eco*RV fragment (nt 1516 to 2247) to make pMD11. The 233-nt *Rsa*I-*Tth*111I fragment (nt 367 to 600) provided an out-of-frame fusion in orfW to serve as a negative control. Upon integration into the *B. subtilis* chromosome at the *sigB* locus—confirmed by Southern blotting—these fusions placed *lacZ* under control of the transcriptional and translational signals of the *sigB* operon.

Mapping the 5′ and 3′ ends of mRNA. RNA was prepared essentially by the method of Igo and Losick (19) with the following modifications. Cultures (25 ml) were grown in 2×SG medium and harvested 2.5 h after the end of exponential growth. Cells were suspended in 2 ml of LETS buffer (19) containing 0.133 ml of vanadyl ribonucleoside complexes (Bethesda Research Laboratories) and lysed by vortexing with glass beads in the presence of 65°C phenol. RNA was extracted again with hot phenol and extracted two times with phenol-chloroform (1:1) and once with chloroform-isoamyl alcohol (24:1). RNA was precipitated by overnight incubation at 4°C with an equal volume of 4 M LiCl (42), washed once in 80% ethanol, and then suspended in 20 μl of diethylpyrocarbonate-treated water (0.2% by volume) containing 40 U of RNasin RNase inhibitor (Promega).

For primer extension reactions to locate the 5′ end of the *sigB* operon message, a 16-base oligomer (Operon Technologies, San Pablo, Calif.) was 5′-end labeled with [γ-^{32}P] dATP (5,000 Ci/mmol; Amersham) and T4 polynucleotide kinase (Boehringer Mannheim). Annealing reactions were done for 3 h at 42°C in a 10-μl volume of 0.02 M Tris (pH 8.3)–0.2 M KCl containing 50 μg of RNA and 5 ng of end-labeled oligomer. Elongation was carried out for 30 min at 42°C by adding the following to the annealing reaction mix: 2 μl of 10× elongation buffer (900 mM Tris [pH 8.3], 100 mM $MgCl_2$, 100 mM dithiothreitol), 2 μl of 2 mM deoxynucleoside 5′-triphosphates, 4.5 μl of water, 0.5 μl of RNasin, and 1 μl of avian myeloblastosis virus reverse transcriptase (12 U/μl; U.S. Biochemicals). Samples were precipitated by adding 1/10 volume of 3 M sodium acetate and 3 volumes of ethanol and then washed once with 80% ethanol. The extended primers were resuspended, heat denatured, and loaded on an 8% polyacrylamide gel containing 8.3 M urea. A sequencing ladder generated by using the same primer with the corresponding pSK12 DNA template served as a standard.

For S1 nuclease protection experiments to locate the 3′ end of the *sigB* operon message, the 259-bp *Eco*RI-*Sau*3A fragment (nt 2293 to 2551 in Fig. 2) was subcloned into the *Eco*RI and *Bam*HI sites of pUC19. This plasmid was 3′-end labeled at the *Eco*RI site, and a 289-bp *Eco*RI-*Hin*dIII fragment containing the 259-bp *Eco*RI-*Sau*3A fragment was gel purified, hybridized with RNA, treated with S1 endonuclease, and then analyzed by electrophoresis on an 8% polyacrylamide gel, as described previously (4).

Enzyme assays. *B. subtilis* cultures were grown to late logarithmic phase and diluted 25:1 into fresh medium to synchronize cell growth. Samples were then taken in both logarithmic and stationary phase and prepared according to the reference cited for each assay. The β-galactosidase assay of Miller (28) was used, with chloroform and sodium dodecyl sulfate to lyse the cells. For catechol 2,3-dioxygenase activities, cell extracts were prepared and the assays were done as described by Ray et al. (33). Chloramphenicol acetyltransferase assays were done by the method of Shaw (39) on extracts of sonicated cells. Protein concentrations for the catechol 2,3-dioxygenase and chloramphenicol acetyltransferase assays were determined with the Bio-Rad protein assay according to the manufacturer's instructions.

Computer analysis. The statistical significance of protein sequence comparisons was evaluated with the FASTP and RDF programs of Lipman and Pearson (25), using the National Biomedical Research Foundation Protein Identification Resource data base and a VAX computer. Sequences considered highly related have an optimized alignment score of greater than 100 and a z value of greater than 10 (25).

Nucleotide sequence accession number. The *sigB* sequence has been assigned GenBank accession no. M34995.

RESULTS

***sigB* operon contains four genes which are expressed in vivo.** Our previous sequence analysis (9) determined that *sigB* was flanked by an upstream open reading frame, orfW, and a downstream, incomplete open reading frame, orfX, encoding a hypothetical protein of at least 20 kilodaltons (kDa). Both the DNA sequence and the lack of promoter activity (see below) suggested that the region initially cloned did not encompass the entire *sigB* operon. We therefore used chromosome-walking methods to isolate adjacent upstream DNA, which was subsequently shown to contain a fourth open reading frame and a sigma-B-dependent promoter for the operon.

As shown in Fig. 1, the 1,029-bp *Eco*RI fragment from λg11-21 (9) was used as a hybridization probe to screen a λgt11 *Eco*RI bank (48) for clone 31. Restriction mapping indicated that clone 31 carried a 2.3-kb *Eco*RI fragment from the *B. subtilis* genome which overlapped the region isolated earlier and which carried an additional 1.3 kb of upstream DNA. The restriction map of this 2.3-kb *Eco*RI fragment was consistent with the map of the region determined by Southern analysis (not shown).

Figure 2 shows the completed sequence extending from the *Pst*I site upstream of orfV to the *Hin*dIII site downstream of orfX. The four open reading frames, in the order orfV-orfW-*sigB*-orfX, encoded hypothetical proteins of 109 residues (12 kDa), 160 residues (18 kDa,) 264 residues (30 kDa), and 199 residues (22 kDa), respectively. The predicted orfV and orfW products were highly acidic, with a calculated pI of 4.70 and 4.29, respectively, and inspection of the DNA sequence indicated that their expression might be translationally coupled, as suggested earlier for the *sigB* and orfX products (9). The orfW and *sigB* reading frames overlapped by 41 nt, and this overlap was preceded by a region of dyad symmetry from nt 890 to 939, a transcript of which has the potential to form a stem-loop with a calculated ΔG of −20.4 kcal (1 cal plus 4.184 J) (9). The significance of this overlap and of the region of symmetry has yet to be determined. All four predicted products had hydropathic profiles typical of soluble proteins. None had obvious DNA-binding motifs save for the *sigB* product, which had the presumptive −10 and −35 contact regions common to most sigma factors (2, 9, 15).

lacZ gene fusions showed that all four frames of the *sigB* operon were translated in vivo. As described in Materials and Methods, we moved fragments with endpoints in each open reading frame to the single-copy, integrational fusion vector pJF751 (11). The fusion reading frame was confirmed by sequencing across the junction between the upstream *B. subtilis* DNA and the site of fusion, the eighth codon of the downstream *lacZ* gene. In order to place each fusion under control of the *sigB* operon regulatory elements, we transformed wild-type *B. subtilis* with selection for chloramphenicol resistance. Southern blotting confirmed that the fusions integrated via Campbell recombination into the chromo-

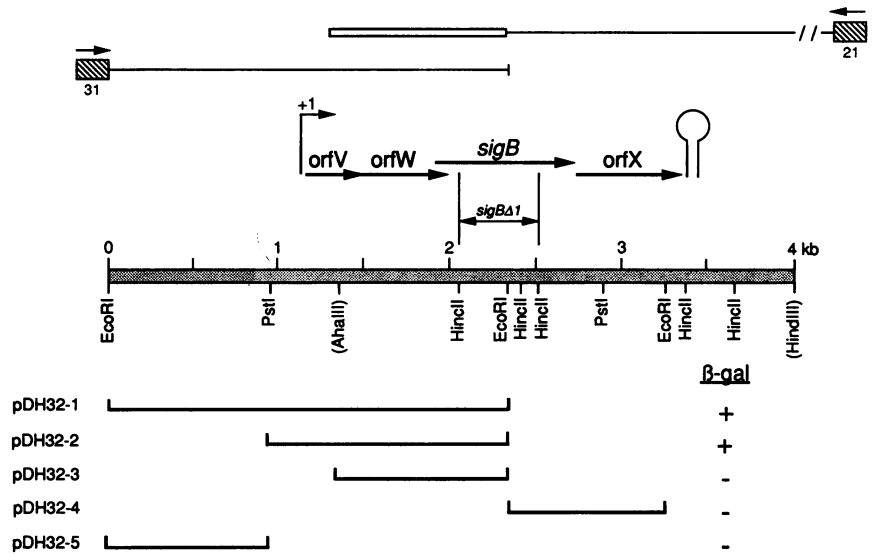

FIG. 1. Physical map of the *sigB* region. The upper portion shows two of the recombinant phages used to derive the restriction map. Phage 21 was isolated previously (9), and phage 31 was isolated in this study. The *lacZ* gene on the right arm of each λgt11 clone is denoted by the hatched box, with the arrow indicating the direction of *lacZ* transcription. The insert of phage 21 is bounded by *Eco*RI linkers inserted during library construction, whereas the insert of phage 31 is bounded by *Eco*RI sites native to the *B. subtilis* genome. The location and direction of transcription of the four open reading frames (orfV, orfW, *sigB*, and orfX) are indicated by arrows above the restriction map, the promoter of the *sigB* operon is shown by the arrow preceding orfV, and the transcription terminator is represented by the stem-loop following orfX. The lines beneath the map show the fragments cloned into the *Eco*RI site of the single-copy transcriptional fusion vector pDH32, oriented so that transcription would extend into the promoterless *lacZ* gene of the vector. These pDH32 constructions were linearized and transformed into the *amyE* locus of *B. subtilis* PB2 *trpC2* and then grown on Schaeffer 2×SG sporulation medium containing 5-bromo-4-chloro-3-indolyl-β-D-galactopyranoside. Fragments having promoter activity are identified by a + in the right column. The map shows only the *Aha*III site at 1.2 kb used for pLC4 fusion constructions and the *Hin*dIII site at 4.0 kb used for DNA sequencing; additional *Aha*III and *Hin*dIII sites are not shown.

somal *sigB* region at the sites shown in Fig. 2. β-Galactosidase assays of cells grown in Schaeffer 2×SG sporulation medium demonstrated that all four fusions were maximally expressed during the early stationary phase of growth (not shown).

These integration events also served as gene disruptions, causing loss of function of the gene disrupted and of downstream genes in the same transcriptional unit (30). Save for the orfX fusion, none of the disruptions had any obvious effect on growth or sporulation in 2×SG sporulation medium. As reported for other orfX null mutations (9, 18), the orfX fusion caused slow growth in rich medium, a small-colony phenotype, and a 10-fold impairment of sporulation.

Similarity between gene products encoded by the *sigB* and *spoIIA* operons. The *B. subtilis spoIIA* operon comprises three genes, *spoIIAA*, *spoIIAB*, and *spoIIAC*, with the *spoIIAC* gene encoding the sporulation-essential sigma-F (13, 30, 45, 49). Developmental mutations mapping to the *spoIIA* locus block sporulation at stage II, 2 h after the end of vegetative growth, when the asymmetric sporulation septum forms and the cell becomes committed to the sporulation process (6, 29). These mutations map in the *spoIIAA* and *spoIIAC* coding regions (53, 54), and the SpoIIAA and SpoIIAC products are thought to act in concert (27). The two known mutations in the *spoIIAB* reading frame increase stationary-phase transcription of *spoIIIG* when cells are grown under nonsporulating conditions (32), and *spoIIIG* in turn codes for the sporulation-essential sigma-G (20, 49).

The organization and primary sequences of the products of the *spoIIA* and *sigB* operons were strikingly similar (Fig. 3A). The 109-residue orfV product had 32% identical residues and 47% conserved substitutions in common with the 117-residue *spoIIAA* product, and the 160-residue orfW product shared 27% identical and 49% conserved residues with the 146-residue *spoIIAB* product. Sigma-B and the *spoIIAC*-encoded sigma-F also had 32% identical residues. The optimized alignments shown in Fig. 3B were highly significant by the alignment score and *z* value criteria of Lipman and Pearson (25). Notably conserved in the orfV product were two glycine residues important for *spoIIAA* function, those defined by the *spoIIAA69* (Gly-62 → Asp) and the *spoIIAA42* (Gly-95 → Asp) mutations (54). Also conserved in the orfW product was the alanine residue altered by the *spoIIAB1* (Ala-11 → Val) mutation (32). The most obvious difference in gene arrangement was the presence of a fourth gene, orfX, following *sigB*. The corresponding position following *spoIIAC* is occupied by the *spoVA* operon (12). The orfX product had no significant similarity to any of the five *spoVA* operon products or to any protein in the Protein Identification Resource data base (Release 23.0).

***lacZ* operon fusions locate promoter activity well upstream of *sigB*.** To locate possible promoters in the *sigB* region, we cloned the fragments shown in Fig. 1 into the single-copy transcriptional fusion vector pDH32 (Dennis Henner, personal communication), which is similar to the *ptrp*BG1 translational fusion vector of Shimotsu and Henner (40). pDH32 carries a split *amyE* gene flanking a chloramphenicol resistance element and a promoterless *spoVG-lacZ* gene fusion. After the fragments were inserted at sites upstream of the fusion, the plasmids were linearized and transformed into *B. subtilis*, integrating by double crossover into the chromosomal *amyE* gene. Southern analyses of these constructs showed that each contained a single copy of the pDH32 derivative at the *amyE* locus. The constructs thus

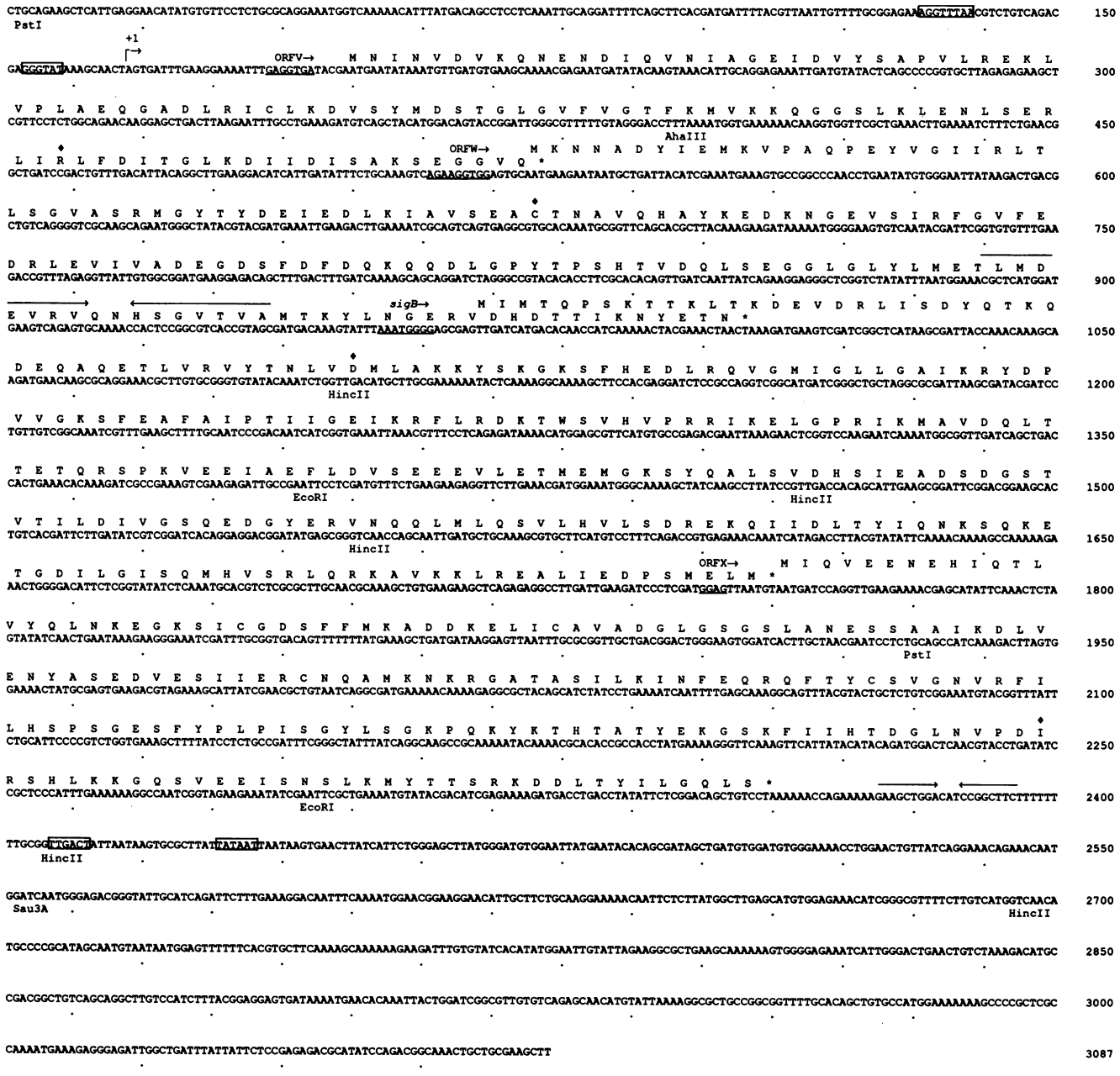

FIG. 2. Nucleotide sequence of the *sigB* operon. Nucleotides are numbered from the 5′ end of the nontranscribed strand, with intervals of 20 bp marked by dots. The sequence of nt 368 to 2297 was reported previously (9) and is included here for clarity. The predicted amino acid sequence for each gene product is given in the single-letter code above the DNA sequence, and the name of each frame is given above the proposed ribosome-binding site (underlined). The proposed −35 and −10 recognition sequences for the sigma-B-dependent *sigB* operon promoter preceding orfV are boxed (nt 131 to 138 and 153 to 158), and regions of symmetry between orfW and *sigB* (nt 890 to 939) and for the proposed *sigB* operon terminator structure following orfX (nt 2368 to 2401) are denoted by the converging arrows. Immediately following the terminator are possible −35 and −10 recognition sequences for sigma-A-containing holoenzyme, also shown boxed (nt 2407 to 2412 and 2431 to 2436), but the downstream sequence encodes no obvious open reading frame. The site of translational fusion of each *sigB* operon reading frame to the eighth codon of *lacZ* carried by the pJF751 vector is indicated (◆). The nucleotide sequence data reported here have been submitted to GenBank and assigned accession number M34995.

carried the transcriptional fusions shown in Fig. 1 inserted at a second site while retaining the intact *sigB* region at its normal chromosomal locus near *dal*.

As shown in Fig. 1, the fusion carrying the entire 2.3-kb *Eco*RI fragment (fragment 1) had promoter activity, as did the *PstI-Eco*RI derivative (fragment 2) lacking 933 bp from the 5′ end of the longer fragment. However, the loss of an additional 366 bp from this region (fragment 3) abolished detectable promoter activity. The 940-bp *Eco*RI fragment (fragment 4) from the 3′ end of the *sigB* region and the 933-bp *Eco*RI-*Pst*I fragment (fragment 5) from the 5′ end of the *sigB* region likewise had no promoter activity under the growth conditions used (Fig. 1). Thus, the major promoter activity in the *sigB* region was localized to the 366-bp region deleted between fragments 2 and 3.

xylE* operon fusions define sequences required for *sigB

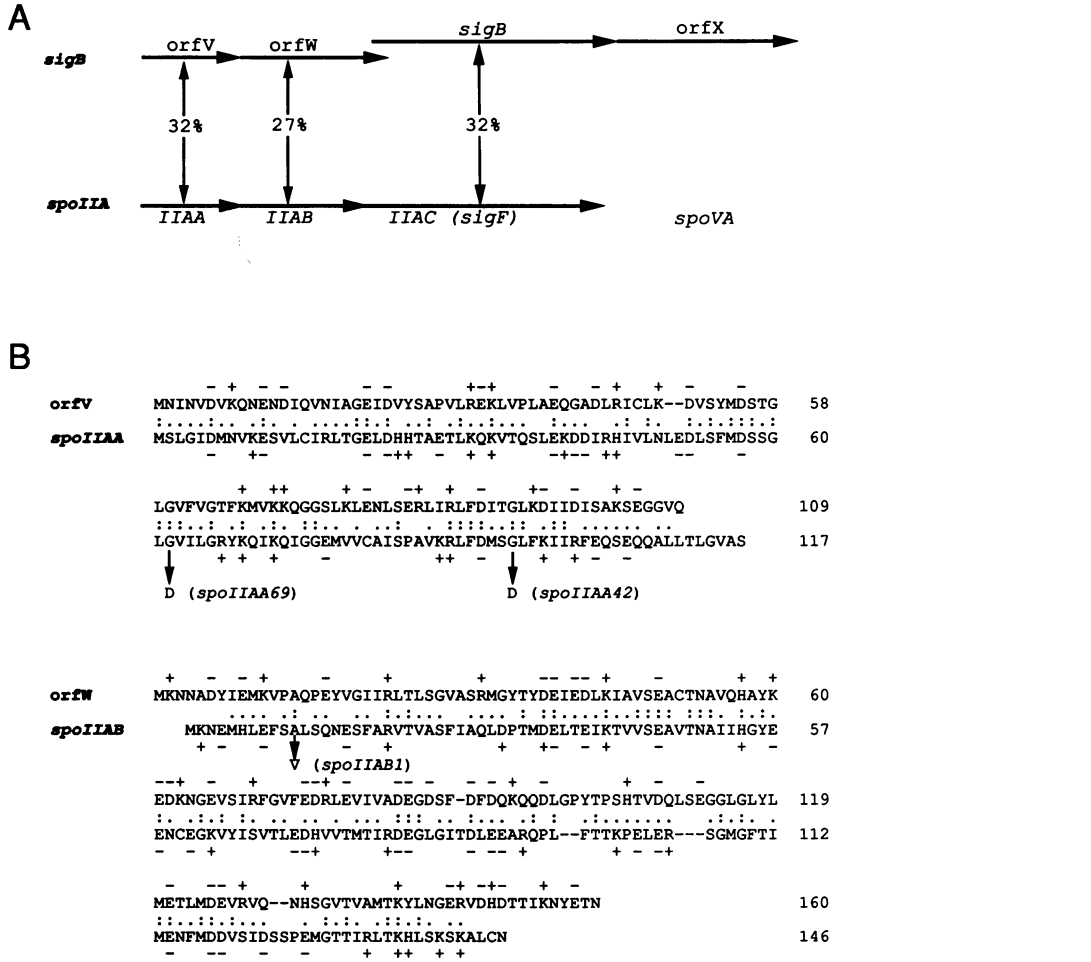

FIG. 3. Similar organization of the *sigB* and *spoIIA* operons. (A) Physical maps of the *sigB* and *spoIIA* operons, with open reading frames indicated by arrows. The *spoIIAC* frame codes for the sporulation-essential sigma-F. Identity between the predicted products of corresponding genes ranges between 27 and 32%, as shown. (B) (Top) FASTP alignment (25) of the 12-kDa orfV and 13-kDa *spoIIAA* products (optimized alignment score, 183; *z* value, 17.0). Residues identical in the two products are denoted by two dots and conserved substitutions (8) by a single dot. Charged residues are designated above and below the lines. Alterations of the *spoIIAA* product that cause a Spo^- phenotype are shown (Gly-62 → Asp and Gly-95 → Asp) (54). (Bottom) FASTP alignment of the 18-kDa orfW and the 16-kDa *spoIIAB* products (optimized alignment score, 154; *z* value, 16.2). The alteration of the *spoIIAB* product that increases *spoIIIG* transcription is shown (Ala-11 → Val) (32). The predicted sequences of the orfV and orfW products are from Fig. 2, and those of the *spoIIAA* and *spoIIAB* products are from Fort and Piggot (13).

operon transcription initiation and termination. The multicopy transcriptional fusion vector pLC4 (33) was used to identify sequences within the 366-bp region that were essential for *sigB* promoter activity. The 397-bp *Pst*I-*Aha*III fragment containing the putative *sigB* promoter region (nt 1 to 397 in Fig. 2) and two 5′ deletions of this fragment (Fig. 4) were separately ligated into the *Eco*RI and *Bam*HI sites upstream of the *xylE* gene of pLC4, and the resultant replicative plasmids were transformed into *B. subtilis* wild-type strain PB2. As shown in Table 2, we determined the catechol 2,3-dioxygenase activity of the three fusion strains as a measure of promoter function. At two points during early stationary phase, the *Pst*I-*Aha*III fragment gave significantly higher activity than the negative control (pLC4 alone), and Δ110 likewise gave good activity. However, Δ139 completely abolished detectable promoter function. As shown in Fig. 4, Δ139 removed sequences to −29, sequences identical to the −35 region of the sigma-B-dependent *ctc* promoter (18, 50).

Immediately following orfX (at nt 2368 to 2401 in Fig. 2) was a sequence similar to that of rho-independent terminators of *E. coli* (35). As a test of terminator function in vivo, we cloned the 117-bp *Eco*RI-*Hin*cII fragment (nt 2293 to 2409) containing the putative terminator into pLC4, between the *sigB* operon promoter carried on the *Pst*I-*Aha*III fragment and the downstream *xylE* reporter gene. As shown in Table 2, this fragment reduced catechol 2,3-dioxygenase activity in pLC400T at least 30-fold, to a level comparable to that of the negative control.

Primer extension and S1 mapping locate the 5′ and 3′ ends of *sigB* mRNA. The primer extension experiment shown in Fig. 5 used a 16-nt primer (complementary to nt 272 to 287 in Fig. 2) to identify the adenine at nt 168 as the 5′ end of the *sigB* operon message. We found the same 5′ end by repeating the primer extension with a 17-nt primer further downstream (complementary to nt 310 to 326; not shown). Thus, *sigB* message either initiated or was processed at nt 168. The *xylE* fusion results described above found that the region

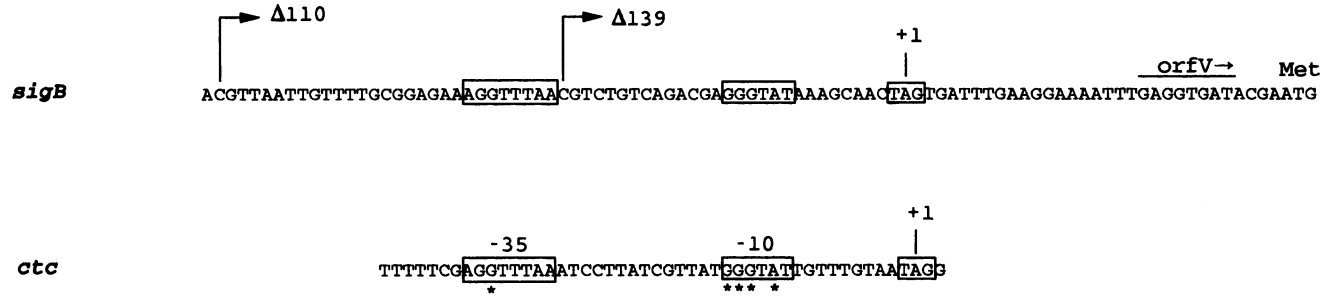

FIG. 4. Comparison of the *sigB* and *ctc* promoter regions. Upper sequence: *sigB* promoter region with the proposed ribosome binding site and initiation codon of the orfV frame shown on the right. The site of transcription initiation, determined by the primer extension experiment shown in Fig. 5, is indicated by +1. Deletions into the promoter region that retain (Δ110) or impair (Δ139) *sigB* promoter activity are shown with the arrow at the 3′ endpoint of the deletion (see Table 2 for results). Boxed sequences in the *sigB* promoter are identical to the recognition sequences of the sigma-B-dependent *ctc* promoter (lower sequence). Mutations at the residues indicated by asterisks significantly decrease *ctc* promoter activity in vitro and in vivo (33, 50).

immediately preceding nt 168 was essential for promoter activity, arguing that nt 168 was the start for the *sigB* message. We have therefore labeled nt 168 as +1 in Fig. 4. Notably, the essential region of the *sigB* operon promoter contained sequences identical to the −10 and −35 regions of the sigma-B-dependent *ctc* promoter (Fig. 4).

S1 mapping located the 3′ end of the *sigB* operon transcript immediately following orfX, within the region similar to rho-independent terminators of *E. coli*. The 259-bp *Eco*RI-*Sau*3A fragment containing this region (nt 2293 to 2551 in Fig. 2) was used as the 3′-end-labeled probe in the experiment shown in Fig. 6. In order to distinguish undigested probe from full-length protection by *B. subtilis* mRNA, the actual probe used in the experiment contained an additional 30 nt from the pUC19 vector. A cluster of protected fragments (98 to 102 nt in length) indicated that the transcript either terminated or was processed between nt 2395 and 2399, within the putative terminator sequence. Because the *xylE* fusion results reported above found that this region had terminator activity in vivo, we consider nt 2395 to 2399 the site of transcription termination for the *sigB* operon. The small amount of fully protected probe shown in Fig. 6 was consistent with the pLC4 results shown in Table 2, indicating that the structure was an efficient terminator in vivo.

Sigma-B is a positive effector and the orfX and *spo0A* products are negative effectors of *sigB* operon transcription.

TABLE 2. Catechol dioxygenase activity in pLC4 transcriptional fusions[a]

Plasmid	Fragment	Catechol dioxygenase sp act (mU/mg of protein)	
		T_{1-2}	T_{2-3}
pLC400	*Pst*I-*Aha*III	6.6	6.6
pLC4Δ110	Δ110	5.8	5.8
pLC4Δ139	Δ139	0.3	0.3
pLC400T	*Pst*I-*Aha*III + terminator	0.2	0.1
pLC4	None (vector alone)	0.4	0.1
pCR31	*ctc* promoter (33)	19.3	14.0

[a]Specific activity in *B. subtilis* PB2 cells containing pLC4 derivatives and grown in 2×SG sporulation medium. Fragments indicated were inserted upstream of the promoterless *xylE* gene of the multicopy vector pLC4. Chloramphenicol acetyltransferase assays (39) confirmed that the copy number of the pLC4 derivatives was essentially the same in all strains (not shown).

We used the single-copy *lacZ* transcriptional fusion pDH32-2 (Fig. 1) as a reporter of the effect of different genetic backgrounds on *sigB* operon transcription. pDH32-2 was transformed into a second site (the *amyE* locus) of the wild-type strain, a *spo0A* mutant, and strains carrying various mutations at the *sigB* locus. pDH32-2 carried fragment 2, encompassing the *sigB* promoter region and extending from the *Pst*I site at nt 1 to the *Eco*RI site at nt 1692, where it joined the vector upstream of the promoterless *lacZ* gene. Since this *Eco*RI site lay within the *sigB* gene, we assume that β-galactosidase activity measured from the fusion at *amyE* reflected the parallel transcription initiating from the same fragment and extending into *sigB* at its normal chromosomal locus near *dal*.

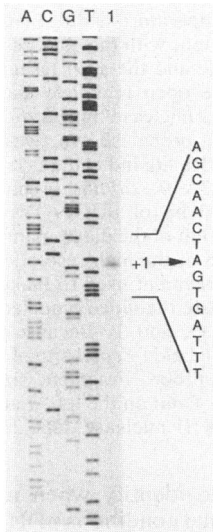

FIG. 5. Mapping the 5′ end of *sigB* operon message by primer extension. The 16-base synthetic primer was complementary to nt 272 to 287, a sequence 118 bp downstream from the transcription start site (+1 in Fig. 2 and 4). Lane 1, End-labeled primer annealed with *B. subtilis* RNA isolated from wild-type PB2 cells at T_2 and extended with reverse transcriptase; lanes A, C, G, and T, dideoxynucleotide sequencing ladder run in parallel with the same primer and the corresponding double-stranded DNA template. The sequence given on the right is the complement of the coding strand. The probable 5′ end of *sigB* message therefore corresponds to the complement of the adenine indicated by +1, because the primer-extended product was phosphorylated and ran slightly faster than the unphosphorylated ladder fragments.

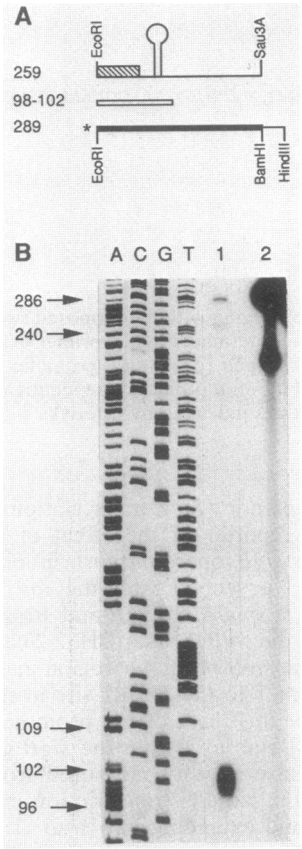

FIG. 6. High-resolution S1 mapping of the 3′ end of the *sigB* message. Reaction conditions were as described previously (4) but with a hybridization temperature of 48°C. (A) (Top) Physical map of the *sigB* terminator region, with the orfX reading frame symbolized by the shaded rectangle and the *sigB* terminator by the stem-loop structure. (Center) The open rectangle shows the portion of the probe protected from S1 nuclease by *B. subtilis* RNA. (Bottom) The 289-bp *Eco*RI-*Hin*dIII probe shown was 3′-end labeled with [α-^{32}P]dATP at the *Eco*RI site indicated (*). The heavy line denotes the 259-bp *Eco*RI-*Sau*3A *B. subtilis* fragment, and the light line shows an additional 30 bp of pUC19 DNA from the polylinker region. Numbers to the left of the diagram indicate fragment sizes (in nt). (B) Autoradiograph of the high-resolution S1 nuclease gel. The 259-bp *Eco*RI-*Sau*3A fragment used to make the probe was cloned into M13mp18 to generate the dideoxynucleotide sequencing ladder shown in lanes A, C, G, and T. Because the sequencing primer began 22 bp before the labeled *Eco*RI site of the probe, the ladder is 22 bp longer than the probe. Fragment sizes (in nt) for selected bands in the A lane are given on the left. Lane 1, Probe plus 120 μg of *B. subtilis* RNA plus S1 nuclease; lane 2, no S1 nuclease.

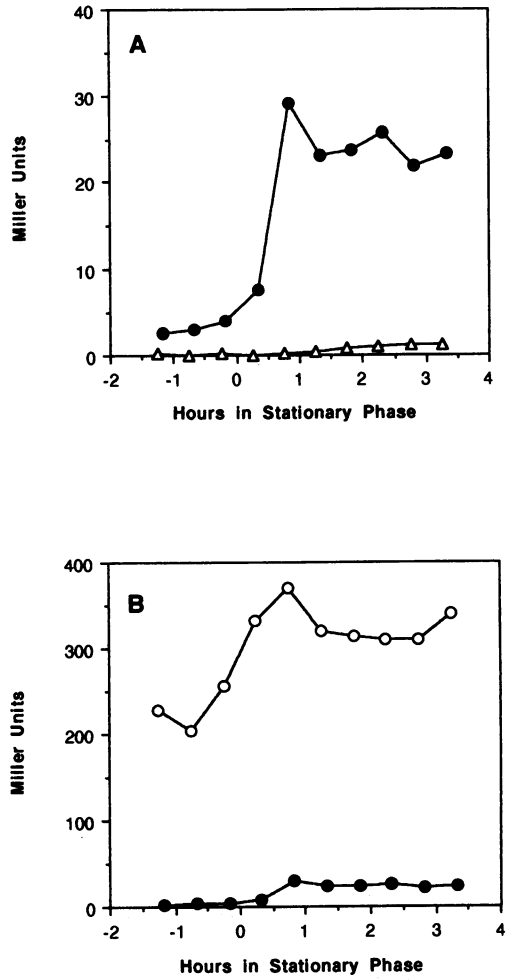

FIG. 7. β-Galactosidase activity of the pDH32-2 *sigB-lacZ* transcriptional fusion in different genetic backgrounds, assayed during growth in Schaeffer 2×SG sporulation medium. T_0 indicates the end of logarithmic growth. (A) Symbols: ●, PB119 (*sigB*$^+$); △, PB122 (*sigBΔ1*). The β-galactosidase activity of PB122 shown was the same as that of the PB120 negative control (not shown). PB120 was a pDH32 integrant strain carrying the same fragment as pDH32-2 but cloned in the opposite orientation to yield pDH32-2R. β-Galactosidase activity in the PB120 negative control never exceeded 2 Miller units at T_3 and has not been subtracted from the curves shown. (B) Symbols: ●, PB119 (orfX$^+$); ○, PB123 (orfX::*ery*). Note that the ordinate has been redrawn from panel A.

We first needed to identify when in the cell cycle and under which nutritional conditions pDH32-2 was most highly expressed. In the experiment shown in Fig. 7A, significant β-galactosidase activity was manifest only after the end of logarithmic growth, reaching a maximum about 1 h into stationary phase (T_1) when cells were grown in 2×SG sporulation medium. Sigma-B-dependent *ctc* transcription also occurs in early stationary phase and is particularly medium dependent, with fivefold-higher expression in LB supplemented with 5.0% glucose and 0.2% glutamine than in nutrient sporulation medium (19). In contrast to *ctc*, we found little difference in expression of the pDH32-2 *sigB* fusion in cells grown in LB supplemented with glucose and glutamine, in unsupplemented LB, in M9 minimal glucose medium, and in 2×SG sporulation medium (data not shown). We used 2×SG for all subsequent characterizations of pDH32-2.

Because essential sequences of the *sigB* promoter were identical to the −10 and −35 regions of the sigma-B-dependent *ctc* promoter, we asked whether transcription of the *sigB* operon was itself dependent on sigma-B. All *sigB* null mutations previously described by us and others are polar on orfX (2, 9, 18). To determine the phenotype of a nonpolar *sigB* mutation, we made a 453-bp in-frame deletion of *sigB* by deleting the 366- and 87-bp *Hin*cII fragments within the *sigB* coding region (Fig. 1). This *sigBΔ1* deletion was inserted into the chromosome by a two-step allele replacement procedure. The *sigB* deletion mutant had no apparent deficiency in a number of sporulation-related or vegetative functions tested (S. Kalman, Ph.D. thesis, Uni-

versity of California, Davis, 1989). However, *sigBΔ1* reduced expression of pDH32-2 to that of the negative control (Fig. 7A), indicating that sigma-B was a positive effector of its own synthesis.

Genetic evidence suggests that the *sigB* and orfX products interact and that the orfX product is a negative effector of *sigB* expression or sigma-B activity (9, 18). As shown in Fig. 7B, a null orfX mutation dramatically enhanced expression of the pHD32-2 fusion during vegetative and stationary-phase growth, confirming that the orfX product was a negative effector of *sigB* expression. Consistent with the fusion results, a primer extension experiment found more *sigB* transcript in the orfX null mutant, and this transcript initiated at the same site in both the mutant and the wild-type strain (not shown). We conclude that the orfX product directly or indirectly affected the level of *sigB* message and thus did control *sigB* expression.

We also tested the effect of a *spo0A* mutation on *sigB* operon expression. The *spo0A* product is a member of the receiver family of two-component regulatory systems and governs many developmental events at the initiation of sporulation as well as a variety of other stationary-phase processes (27, 41). In contrast to most developmental and stationary-phase genes which require Spo0A as a positive effector, Igo and Losick (19) found that Spo0A was a negative effector of the sigma-B-dependent expression of *ctc*. To determine whether expression of the *sigB* operon itself was affected by the *spo0A* product, we assayed the pDH32-2 transcriptional fusion in a strain carrying the *spo0A12* nonsense mutation and found a twofold enhancement of β-galactosidase activity (data not shown). Thus, Spo0A had a modest negative effect on *sigB* expression, similar to its effect on *ctc*.

DISCUSSION

Little is known about the detailed mechanisms by which metabolic, environmental, and morphological signals are transmitted to the *B. subtilis* transcriptase to effect changes in gene expression. Here we identify factors that regulate sigma-B, an alternate sigma factor which controls genes expressed in the early stationary phase of growth. We have shown that the sigma-B structural gene lies in an operon with surprisingly complex regulation and, furthermore, that the genetic organization of this operon is unexpectedly similar to that of the sporulation-essential *spoIIA* operon.

The *sigB* operon comprised at least four genes in the order orfV-orfW-*sigB*-orfX (Fig. 1). Single-copy *lacZ* translational fusions showed that all four products were translated in vivo and that none were essential for growth or sporulation in rich or minimal medium. The operon was closely bounded by promoter and terminator regions, which were defined both by function and by mapping the 5′ and 3′ ends of in vivo message.

Our most striking result was the significant similarity of the orfV, orfW, and *sigB* products to their counterpart *spoIIAA*, *spoIIAB*, and *spoIIAC* products, respectively, in the *spoIIA* operon (Fig. 3). The *spoIIAC* gene encodes sigma-F, the precise role of which remains to be identified but which is required for the sporulation process to proceed past stage II (13, 27, 45, 49). These similarities in product sequence and overall genetic organization are shared by no other sigma factor operon so far characterized. We infer from these results that an evolutionary relationship exists between the two operons, which lie directly opposite each other on the *B. subtilis* genetic map and may thus have arisen as a tandem duplication of an ancestral chromosome (34). From this clear evolutionary relationship, and from the fact that both operons are expressed during the early stationary phase of growth (Fig. 7) (10, 38, 51), we speculate that two possible levels of functional relationship might exist between them.

First, the following considerations lead us to theorize that the 12- to 13-kDa orfV-*spoIIAA* and 16- to 18-kDa orfW-*spoIIAB* products function by a common molecular mechanism to regulate expression or activity of their respective sigma factors or to coordinate expression of a related pathway. (i) Based on the phenotypes of *spoIIAA* and *spoIIAC* mutants, the *spoIIAA* product is thought to act positively with sigma-F to regulate formation of the asymmetric sporulation septum. This septum divides the cell into forespore and mother cell compartments, an event critical for proper execution of the developmental program (27, 29). (ii) Mutations within the *spoIIAB* reading frame increase stationary-phase expression of a *spoIIIG-lacZ* fusion when cells are grown under nonsporulating conditions, leading Moran and his colleagues to suggest that SpoIIAB negatively regulates *spoIIIG*, the gene for the forespore-specific sigma-G (32). (iii) The OrfV-SpoIIAA and OrfW-SpoIIAB alignments are remarkably alike (Fig. 3), and residues important for SpoIIAA and SpoIIAB function are conserved within OrfV and OrfW, respectively. (iv) Both the orfV-orfW and *spoIIAA-spoIIAB* reading frames have overlapping termination and initiation codons, with identical sequences at the junction of each (Fig. 2) (12). Thus, expression of the products of each gene pair may be translationally coupled, presumably to ensure equimolar synthesis of proteins which act together in vivo. The question of whether these paired products form a regulatory system and the level at which they act can be addressed by determining the effect of orfV and orfW null mutations on expression from the sigma-B-dependent *ctc* and *csbA* promoters (18; S. A. Boylan, M. D. Thomas, and C. W. Price, unpublished data).

The second possible physiological link between the two operons is more speculative still: we imagine that the *sigB* and *spoIIA* operons might regulate divergent branches of stationary-phase metabolism. Given one signal, the cell chooses the *spoIIA* pathway, leading to spore formation. But given another, as yet unknown signal, the cell chooses the *sigB* pathway, leading to a different fate. It is equally possible that the two operons retain no physiological link but use an equivalent mechanism to perform unrelated roles. These alternatives can be addressed by establishing the functions of genes constituting the sigma-B and sigma-F regulons and by establishing which signals regulate the two operons.

A clear difference between the operons is the autoregulation of *sigB* expression by both sigma-B and the orfX product, which has no counterpart in the *spoIIA* operon. Developmental transcription of the *spoIIA* operon principally initiates 27 nt upstream from the *spoIIAA* coding sequence and is dependent upon the unlinked *spo0H* gene, which encodes the sporulation-essential sigma-H (51). We used *lacZ* transcriptional fusions in the single-copy vector pDH32 to find the only promoter activity in the *sigB* region in a corresponding location, just upstream of orfV (Fig. 1). Primer extension experiments mapped the 5′ end of *sigB* operon message to nt 168, 32 nt upstream from the putative orfV translational initiation codon (Fig. 3 and 4), and experiments with the multicopy vector pLC4 confirmed that sequences directly preceding nt 168 were necessary for promoter activity in vivo (Fig. 4 and Table 2). Together,

these results defined the region between nt 1 and 397 as a major promoter for the *sigB* operon.

The promoter-distal gene pair of the operon, *sigB* and orfX, autoregulated expression at this promoter, the presumptive −10 and −35 sequences of which were identical to those of the sigma-B-dependent *ctc* promoter. Because a *sigB* deletion reduced expression of the *sigB-lacZ* transcriptional fusion pDH32-2 to imperceptible levels, sigma-B is formally a positive factor required for its own synthesis. The simplest explanation for these results is that transcription initiating at nt 168 was mediated by sigma-B-containing holoenzyme. Such an autocatalytic circuit would allow rapid synthesis of sigma-B once the operon was derepressed, perhaps by inactivating the orfX product, and would also provide a rapid homeostatic control to equalize new steady-state levels of sigma-B synthesis.

Two other sigma factors, sigma-G and sigma-K, are also thought to positively control their own synthesis (20, 21). Both are essential for sporulation and are thought to govern compartment-specific gene expression in the forespore and mother cell, respectively (20, 21, 46, 49). The genes for sigma-G and sigma-K appear to be expressed initially via readthrough transcription from upstream operons, thereby ensuring the presence of sufficient sigma factor to permit the autocatalytic induction (20, 21).

Our preliminary results suggest that the *sigB* operon might also be partly transcribed via readthrough from upstream. The *lacZ* translational fusions made by integrating the pJF751 vector into the orfV, orfW, and *sigB* reading frames were polar gene disruptions which should block sigma-B synthesis (Fig. 1), yet these fusions were themselves expressed, arguing for the existence of a second promoter transcribed by an activity other than sigma-B holoenzyme. On the basis of the high level of expression of these translational fusions (not shown), this second promoter provides significant levels of *sigB* operon message. Two results suggest that this second promoter lay upstream from the *Eco*RI site at 0 kb in Fig. 1, beyond the region cloned. First, transcription initiating from near nt 168—measured by *lacZ* fusion activity (Fig. 7) and by primer extension (not shown)—was undetectable in the *sigB* null mutant. Thus, the second holoenzyme form most likely initiates transcription at a site distinct from the sigma-B-dependent start at nt 168. Second, our transcriptional fusion results found no other significant promoter activity elsewhere in the region upstream of orfV (Fig. 1). Additional experiments will be needed to determine the physiological importance of transcription into the *sigB* operon from this presumed upstream promoter.

The available data indicate that the orfX product is formally a negative regulator of *sigB* operon expression. We found earlier that mutations within the orfX frame caused a small-colony phenotype only in the presence of an intact *sigB* locus, suggesting an interaction between the orfX and *sigB* products in vivo (9). Furthermore, the *socB* mutation, isolated on the basis of its increased expression of a *ctc-xylE* fusion, proved to be a frameshift within the orfX reading frame (18). Together, these results suggested that the orfX product—or the product of a downstream gene in the same transcriptional unit—was a negative effector of *sigB* expression or activity.

The results reported here show that the orfX product was directly or indirectly responsible for this regulation, and the transcriptional fusion results suggest that the orfX product negatively affected the level of message initiating from the *sigB* operon promoter. However, the mechanism by which the orfX product influenced *sigB* message levels remains to be established. Because sigma-B was a positive effector of its own synthesis, we cannot distinguish whether elevated *sigB* expression in the orfX mutant was due to increased synthesis of sigma-B or increased activity of sigma-B holoenzyme. If synthesis of sigma-B and the orfX product is translationally coupled, as implied by the arrangement of their coding sequences (9), we hypothesize that their products are required in equimolar amounts. We therefore currently favor a model in which the orfX product, in response to an as yet unknown signal, modulates sigma-B activity by its association either with sigma-B holoenzyme or with free sigma-B. According to this model, an orfX null mutation would elevate expression of the sigma-B-dependent *ctc* gene (18) primarily by increasing sigma-B activity and secondarily by increasing sigma-B synthesis as a result of the autocatalytic nature of *sigB* expression.

Regulation of the *sigB* operon appears to be elaborate, with at least two possible routes of information entry, through orfX and through the orfV-orfW pair. Further analysis will establish the mechanism of orfX regulation and the function of the orfV and orfW products. Isolation and characterization of additional genes in the sigma-B regulon should establish the physiological function of the pathway controlled by sigma-B.

ACKNOWLEDGMENTS

We thank Susan Fisher for providing the primer extension protocol, Dennis Henner for pDH32, and Charles Moran for pLC4. We particularly thank Alan Grossman for his helpful comments on the manuscript.

This research was supported by Public Health Service grant GM42077 from the National Institute of General Medical Sciences to C.W.P. and by a Jastro-Shields Graduate Research Award to S.K.

LITERATURE CITED

1. **Arnosti, D. N., and M. J. Chamberlin.** 1989. Secondary σ factor controls transcription of flagellar and chemotaxis genes in *Escherichia coli*. Proc. Natl. Acad. Sci. USA **86**:830–834.
2. **Binnie, C., M. Lampe, and R. Losick.** 1986. Gene encoding the sigma-37 species of RNA polymerase sigma factor from *Bacillus subtilis*. Proc. Natl. Acad. Sci. USA **83**:5943–5947.
3. **Boylan, S. A., K. T. Chun, B. A. Edson, and C. W. Price.** 1988. Early-blocked sporulation mutations alter expression of enzymes under carbon control in *Bacillus subtilis*. Mol. Gen. Genet. **212**:271–280.
4. **Boylan, S. A., J.-W. Suh, S. M. Thomas, and C. W. Price.** 1989. Gene encoding the alpha core subunit of *Bacillus subtilis* RNA polymerase is cotranscribed with the genes for initiation factor 1 and ribosomal proteins B, S13, S11, and L17. J. Bacteriol. **171**:2553–2562.
5. **Chater, K. F., C. J. Bruton, K. A. Plaskitt, M. J. Buttner, C. Mendez, and J. D. Helmann.** 1989. The developmental fate of *S. coelicolor* hyphae depends upon a gene product homologous with the motility σ factor of *B. subtilis*. Cell **59**:133–143.
6. **Cooney, P. H., P. F. Whiteman, and E. Freese.** 1977. Media dependence of commitment in *Bacillus subtilis*. J. Bacteriol. **129**:901–907.
7. **Davis, R. W., D. Botstein, and J. R. Roth.** 1980. Advanced bacterial genetics; a manual for genetic engineering. Cold Spring Harbor Laboratory, Cold Spring Harbor, N.Y.
8. **Dayhoff, M. D., R. M. Schwartz, and B. C. Orcutt.** 1978. A model of evolutionary change in proteins, p. 345–352. *In* M. D. Dayhoff (ed.), Atlas of protein sequence and structure, vol. 5, suppl. 3. National Biomedical Research Foundation, Silver Spring, Md.
9. **Duncan, M. L., S. S. Kalman, S. M. Thomas, and C. W. Price.** 1987. Gene encoding the 37,000-dalton minor sigma factor of *Bacillus subtilis* RNA polymerase: isolation, nucleotide se-

quence, chromosomal locus, and cryptic function. J. Bacteriol. **169**:771–778.
10. **Errington, J., and J. Mandelstam.** 1986. Use of a *lacZ* gene fusion to determine the dependence pattern of sporulation operon *spoIIA* in *spo* mutants of *Bacillus subtilis*. J. Gen. Microbiol. **132**:2967–2976.
11. **Ferrari, F. A., K. Trach, and J. A. Hoch.** 1985. Sequence analysis of the *spo0B* locus reveals a polycistronic transcriptional unit. J. Bacteriol. **161**:556–562.
12. **Fort, P., and J. Errington.** 1985. Nucleotide sequence and complementation analysis of a polycistronic sporulation operon, *spoVA*, in *Bacillus subtilis*. J. Gen. Microbiol. **131**:1091–1105.
13. **Fort, P., and P. J. Piggot.** 1984. Nucleotide sequence of sporulation locus *spoIIA* in *Bacillus subtilis*. J. Gen. Microbiol. **206**:579–590.
14. **Grossman, A. D., J. W. Erickson, and C. A. Gross.** 1984. The *htpR* gene product of *E. coli* is a sigma factor for heat shock promoters. Cell **38**:383–390.
15. **Helmann, J. D., and M. J. Chamberlin.** 1988. Structure and function of bacterial sigma factors. Annu. Rev. Biochem. **57**: 839–872.
16. **Helmann, J. D., L. M. Marquez, and M. J. Chamberlin.** 1988. Isolation and characterization of the *Bacillus subtilis* σ^{28} gene. J. Bacteriol. **170**:1560–1567.
17. **Horinouchi, S., and B. Weisblum.** 1982. Nucleotide sequence and functional map of pE194, a plasmid that specifies inducible resistance to macrolide, lincosamide, and streptogramin type B antibiotics. J. Bacteriol. **150**:804–814.
18. **Igo, M., M. Lampe, C. Ray, W. Shafer, C. P. Moran, and R. Losick.** 1987. Genetic studies of a secondary RNA polymerase sigma factor in *Bacillus subtilis*. J. Bacteriol. **169**:3464–3469.
19. **Igo, M., and R. Losick.** 1986. Regulation of a promoter that is utilized by minor forms of RNA polymerase holoenzyme in *Bacillus subtilis*. J. Mol. Biol. **191**:615–624.
20. **Karmazyn-Campelli, C., C. Bonamy, B. Savelli, and P. Stragier.** 1989. Tandem genes encoding σ-factors for consecutive steps of development in *Bacillus subtilis*. Genes Dev. **3**:150–157.
21. **Kroos, L., B. Kunkel, and R. Losick.** 1989. Switch protein alters specificity of RNA polymerase containing a compartment-specific sigma factor. Science **243**:526–529.
22. **Kustu, S., E. Santero, J. Keener, D. Popham, and D. Weiss.** 1989. Expression of σ^{54} (*ntrA*)-dependent genes is probably united by a common mechanism. Microbiol. Rev. **53**:367–376.
23. **Landick, R., V. Vaughn, E. T. Lau, R. A. VanBogelen, J. W. Erickson, and F. C. Neidhardt.** 1984. Nucleotide sequence of the heat shock regulatory gene of *E. coli* suggests its protein product may be a transcription factor. Cell **38**:175–182.
24. **Leighton, T. J., and R. H. Doi.** 1971. The stability of messenger ribonucleic acid during sporulation in *Bacillus subtilis*. J. Biol. Chem. **252**:268–272.
25. **Lipman, D. J., and W. R. Pearson.** 1985. Rapid and sensitive protein similarity searches. Science **227**:1435–1441.
26. **Losick, R., and J. Pero.** 1981. Cascades of sigma factors. Cell **25**:582–584.
27. **Losick, R., P. Youngman, and P. J. Piggot.** 1986. Genetics of endospore formation in *Bacillus subtilis*. Annu. Rev. Genet. **20**:625–670.
28. **Miller, J. H.** 1972. Experiments in molecular genetics. Cold Spring Harbor Laboratory, Cold Spring Harbor, N.Y.
29. **Piggot, P. J., and J. G. Coote.** 1976. Genetic aspects of bacterial endospore formation. Bacteriol. Rev. **40**:908–962.
30. **Piggot, P. J., C. A. M. Curtis, and H. DeLencastre.** 1984. Use of integrational plasmid vectors to demonstrate the polycistronic nature of a transcriptional unit (*spoIIA*) required for sporulation of *Bacillus subtilis*. J. Gen. Microbiol. **130**:2123–2136.
31. **Price, C. W., and R. H. Doi.** 1985. Genetic mapping of *rpoD* implicates the major sigma factor of *Bacillus subtilis* RNA polymerase in sporulation initiation. Mol. Gen. Genet. **210**: 88–95.
32. **Rather, P. N., R. Coppolecchia, H. DeGrazia, and C. P. Moran.** 1990. Negative regulator of σ^{G}-controlled gene expression in stationary-phase *Bacillus subtilis*. J. Bacteriol. **172**:709–715.
33. **Ray, C., R. E. Hay, H. L. Carter, and C. P. Moran.** 1985. Mutations that affect utilization of a promoter in stationary-phase *Bacillus subtilis*. J. Bacteriol. **163**:610–614.
34. **Riley, M., L. Soloman, and D. Zipkas.** 1978. Relationship between gene function and gene location in *Escherichia coli*. J. Mol. Evol. **11**:47–56.
35. **Rosenberg, M., and D. Court.** 1979. Regulatory sequences involved in the promotion and termination of RNA transcription. Annu. Rev. Genet. **13**:13:319–353.
36. **Sala-Trepat, J., and W. C. Evans.** 1971. The meta cleavage of catechol by *Azotobacter* species 4-oxalocrotonate pathway. Eur. J. Biochem. **20**:400–413.
37. **Sanger, F., S. Nicklen, and A. R. Coulson.** 1977. DNA sequencing with chain-terminating inhibitors. Proc. Natl. Acad. Sci. USA **74**:5463–5467.
38. **Savva, D., and J. Mandelstam.** 1986. Synthesis of *spoIIA* and *spoVA* mRNA in *Bacillus subtilis*. J. Gen. Microbiol. **132**: 3005–3011.
39. **Shaw, W. V.** 1975. Chloramphenicol acetyltransferase from chloramphenicol-resistant bacteria. Methods Enzymol. **43**: 737–755.
40. **Shimotsu, H., and D. J. Henner.** 1986. Construction of a single-copy integration vector and its use in analysis of the *trp* operon of *Bacillus subtilis*. Gene **43**:85–94.
41. **Sonenshein, A. L.** 1989. Metabolic regulation of sporulation and other stationary-phase phenomena, p. 109–130. *In* I. Smith, R. A. Slepecky, and P. Setlow (ed.), Regulation of procaryotic development. American Society for Microbiology, Washington, D.C.
42. **Sripati, C. E., and J. R. Warner.** 1978. Isolation, characterization, and translation of mRNA from yeast. Methods Cell Biol. **20**:61–81.
43. **Stahl, M. L., and E. Ferrari.** 1984. Replacement of the *Bacillus subtilis* subtilisin structural gene with an in vitro-derived mutation. J. Bacteriol. **158**:411–418.
44. **Stock, J., A. J. Ninfa, and A. M. Stock.** 1989. Protein phosphorylation and regulation of adaptive responses in bacteria. Microbiol. Rev. **53**:450–490.
45. **Stragier, P.** 1986. Comment on "Duplicated sporulation genes in bacteria" by J. Errington, P. Fort, and J. Mandelstam (FEBS Lett. **188**:184–185, 1985). FEBS Lett. **195**:9–11.
46. **Stragier, P., B. Kunkel, L. Kroos, and R. Losick.** 1989. Chromosomal rearrangement generating a composite gene for a developmental transcription factor. Science **243**:507–512.
47. **Straus, D. B., W. A. Walter, and C. Gross.** 1987. The heat shock response of *E. coli* is regulated by changes in the concentration of σ^{32}. Nature (London) **329**:348–351.
48. **Suh, J.-W., S. A. Boylan, and C. W. Price.** 1986. Gene for the alpha subunit of *Bacillus subtilis* RNA polymerase maps in the ribosomal protein gene cluster. J. Bacteriol. **168**:65–71.
49. **Sun, D., P. Stragier, and P. Setlow.** 1989. Identification of a new sigma factor involved in compartmentalized gene expression during sporulation of *Bacillus subtilis*. Genes Dev. **3**:141–149.
50. **Tatti, K. M., and C. P. Moran, Jr.** 1984. Promoter recognition by sigma-37 RNA polymerase from *Bacillus subtilis*. J. Mol. Biol. **175**:285–297.
51. **Wu, J.-J., M. G. Howard, and P. J. Piggot.** 1989. Regulation of transcription of the *Bacillus subtilis spoIIA* locus. J. Bacteriol. **171**:692–698.
52. **Young, R. A., and R. W. Davis.** 1983. Yeast RNA polymerase II genes: isolation with antibody probes. Science **222**:778–783.
53. **Yudkin, M. D.** 1987. Structure and function in a *Bacillus subtilis* sporulation-specific sigma factor. J. Gen. Microbiol. **133**: 475–481.
54. **Yudkin, M. D., K. A. Jarvis, S. E. Raven, and P. Fort.** 1985. Effects of transition mutations in the regulatory locus *spoIIA* on the incidence of sporulation in *Bacillus subtilis*. J. Gen. Microbiol. **131**:959–962.